J|A|C|S
ARTICLES
Published on Web 06/12/2002

Reactivity and Selectivity of the *N*-Acetyl-Glu-P-1, *N*-Acetyl-Glu-P-2, *N*-Acetyl-MeIQx, and *N*-Acetyl-IQx Nitrenium Ions: Comparison to Carbocyclic *N*-Arylnitrenium Ions

Michael Novak,* Krisztina Toth, Sridharan Rajagopal, Michael Brooks, Lora L. Hott, and Matthew Moslener

Contribution from the Department of Chemistry and Biochemistry, Miami University, Oxford, Ohio 45056

Received September 18, 2001. Revised Manuscript Received April 29, 2002

Abstract: The model ultimate carcinogens **1a**−**d**, related to the metabolites of the food-derived carcinogenic heterocyclic amines **Glu-P-1**, **Glu-P-2**, **MeIQx**, and **IQx**, spontaneously decompose in neutral aqueous solution to generate the heterocyclic nitrenium ions, **2a**−**d**. The less reactive esters **1a** and **1b** also undergo acid-catalyzed ester hydrolysis to generate the corresponding hydroxamic acids at pH <2, while the more reactive **2c** and **2d** are prone to rearrangement in nonaqueous solvents. The reactions of the nitrenium ions with AcO^-, HPO_4^{2-}, N_3^-, and 2′-deoxyguanosine (d-G) were characterized in aqueous solution by using a combination of competitive trapping methods and product isolation and identification. The reactions with N_3^- and d-G generally follow patterns previously established for carbocyclic nitrenium ions, but the reactions with AcO^- and HPO_4^{2-} are unusual. Similar reactions have previously only been reported for heterocyclic 1-alkyl-2-imidazolium ions. The N_3^-/solvent selectivities of these ions (5.1×10^6 M^{-1} for **2a**, 2.3×10^6 M^{-1} for **2b**, 1.2×10^5 M^{-1} for **2c**, and 5.2×10^4 M^{-1} for **2d**) are comparable to those of highly selective carbocyclic nitrenium ions. If k_{az} for these ions is diffusion limited at ca. 5×10^9 M^{-1} s^{-1} the aqueous solution lifetimes of these ions range from 10 μs (**2d**) to 1 ms (**2a**). These ions are also highly selective for trapping by d-G, but comparisons to other nitrenium ions show that they are 10- to 50-fold less selective for trapping by d-G than they would be if both the N_3^- and d-G reactions were diffusion limited. This is not a consequence of their heterocyclic structures. Several carbocyclic ions show similar behavior. The relatively inefficient trapping of **2c** and **2d** by d-G may account for the observation of the unusual minor N-2 d-G adduct that is isolated for both of these nitrenium ions, but has not previously been observed for the reactions of other nitrenium ions with monomeric d-G.

Introduction

Mutagenic and carcinogenic heterocyclic amines (HCAs) are found in parts per billion concentrations in broiled and fried meats and other protein-containing foods, as well as in tobacco smoke.[1] A list of selected carcinogenic HCAs is presented in Scheme 1 along with the common metabolic pathway required for activation into their ultimate carcinogenic forms, the sulfuric or acetic acid esters of the corresponding hydroxylamines.[1,2] The HCAs are classified structurally into two groups: the IQ type HCAs that are characterized by an imidazoquinoline, imidazoquinoxaline, or related structure, and the non-IQ type HCAs that are typically characterized by a 2-aminopyridine structure.[1] We have previously shown that ester derivatives of two of the more weakly mutagenic non-IQ HCAs, **Phe-P-1** and **AαC**, decompose in aqueous solution to generate nitrenium ions with low to moderate N_3^-/solvent selectivity measured as k_{az}/k_s, the ratio of the second-order rate constant for N_3^- trapping of the nitrenium ion and the pseudo-first-order rate constant for trapping the ion by the aqueous solvent.[3,4]

Glu-P-1, **Glu-P-2**, **IQx**, and **MeIQx** are synthetically easily accessible examples of the more highly mutagenic and carci-

* Corresponding author. E-mail: novakm@muohio.edu. Phone: 513-529-2813. Fax: 513-529-5715.

(1) Eisenbrand, G.; Tang, W. *Toxicology* **1993**, *84*, 1−82. Hatch, F. T.; Knize, M. G.; Felton, J. S. *Environ. Mol. Mutagen.* **1991**, *17*, 4−19. Layton, D. W.; Bogen, K. T.; Knize, M. G.; Hatch, F. T.; Johnson, V. M.; Felton, J. S. *Carcinogenesis* **1995**, *16*, 39−52. Sugimura, T. *Environ. Health Perspect.* **1986**, *67*, 5−10.

(2) Sugimura, T. *Mutat. Res.* **1985**, *150*, 33−41. Felton, J. S.; Knize, M. G.; Shen, N. H.; Anderson, B. D.; Bjeldames, L. F.; Hatch, F. T. *Environ. Health Perspect.* **1986**, *67*, 17−24. Hashimoto, Y.; Shudo, K.; Okamoto, T. *Acc. Chem. Res.* **1984**, *17*, 403−408. Shinohara, A.; Saito, K.; Yamazoe, Y.; Kamataki, T.; Kato, R. *Cancer Res.* **1986**, *46*, 4362−4367. Aoyama, T.; Gonzalez, F. J.; Gelboin, H. V. *Mol. Carcinogen.* **1989**, *2*, 192−198. Snyderwine, E. G.; Wirth, P. J.; Roller, P. P.; Adamson, R. H.; Sato, S.; Thorgiersson, S. S. *Carcinogenesis* **1988**, *9*, 411−418. Meerman, J. H. N.; Ringer, D. P.; Coughtrie, M. W. H.; Bamforth, K. J.; Gilissen, R. A. H. J. *Chem.-Biol. Interact.* **1994**, *92*, 321−328. Raza, H.; King, R. S.; Squires, R. B.; Guengerich, F. P.; Miller, D. W.; Freeman, J. P.; Lang, N. P.; Kadlubar, F. F. *Drug Metab. Dispos.* **1996**, *24*, 385−400. Watanabe, M.; Ishidate, M.; Nobmi, T. *Mutat. Res.* **1990**, *234*, 337−348. Wakabayashi, K.; Nagao, M.; Esumi, H.; Sugimura, T. *Cancer Res.* **1992**, *52*, 2 (Suppl.), 2092s−2098s. Turesky, R. J.; Bracco-Hammer, I.; Markovic, J.; Richli, U.; Kappeler, A.-M.; Welti, D. H. *Chem. Res. Toxicol.* **1990**, *3*, 524−535. Turesky, R. J.; Markovic, J.; Bracco-Hammer, I.; Fay, L. B. *Carcinogenesis* **1991**, *12*, 1847−1855. Rich, K. J.; Murray, B. P.; Lewis, I.; Rendell, N. B.; Davies, D. S.; Gooderham, N. J.; Boobis, A. R. *Carcinogenesis* **1992**, *13*, 2221−2226. Snyderwine, E. G.; Schut, H. A. J.; Adamson, R. H.; Thorgeirsson, U. P.; Thorgeirsson, S. S. *Cancer Res.* **1992**, *52* (Suppl.) 2099s−2102s. Schut, H. A. J.; Snyderwine, E. G. *Carcinogenesis* **1999**, *20*, 353−368.

(3) Novak, M.; Xu, L.; Wolf, R. A. *J. Am. Chem. Soc.* **1998**, *120*, 1643−1644.

10.1021/ja0121944 CCC: $22.00

Scheme 1

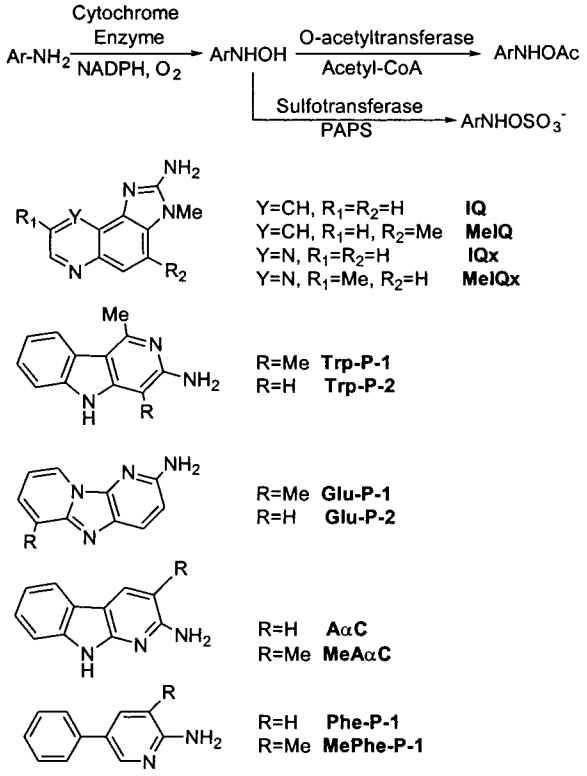

nogenic members of both structural groups. **Glu-P-1** and **Glu-P-2** are pyrolysis products of glutamic acid.[1] They have been detected in the pyrolysis mixtures of casein,[5] in the oil of charred egg yolk, a commercial food product in Japan,[6] and in Worcestershire sauce,[7] among other sources.[1] **IQx** and **MeIQx** are products of the reaction of amino acids, reducing sugars, and creatine at temperatures above 100 °C.[1] They are found in broiled and fried meats and fish, and derived products such as beef extract and bouillon cubes.[1]

These amines cause cancers in the livers, small and large intestines, forestomachs, and other organs of laboratory rats and mice, and are presumed human carcinogens.[1] **Glu-P-1** binds to DNA in the presence of rat liver microsomes to form the familiar C-8 guanine adduct common to a wide variety of carbocyclic and heterocyclic arylamines.[1,8] **MeIQx** generates both the C-8 adduct and the less commonly observed N-2 adduct.[9]

In this paper we present results of our study of the hydrolysis reactions of **1a**−**d** and of the subsequent chemistry of the nitrenium ions **2a**−**d** (Scheme 2). The esters **1a**−**d** are acetic acid esters of the *N*-acetylhydroxamic acid derivatives of the four amines. It would be preferable to have data for the acetic acid esters of the corresponding hydroxylamines, **3a**−**d**, since these are the putative carcinogens. Both **3a** and **3b** have been synthesized in situ for DNA modification studies, but were not isolated.[10] Syntheses of **3c** and **3d** have not been reported. We

Scheme 2

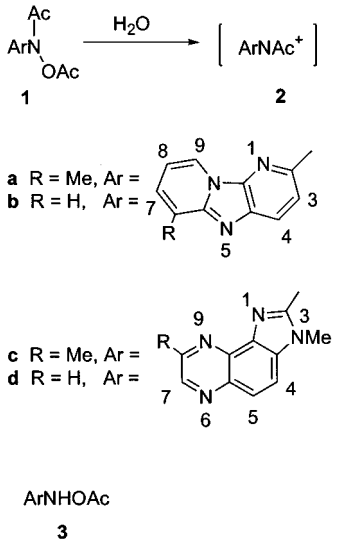

have not been able to isolate **3a**−**d** presumably because of their high reactivity with H_2O. Our previous studies have shown that the *N*-acetyl group of the hydroxamic acid esters can stabilize the esters toward hydrolysis by N−O bond heterolysis by a factor of 5×10^3−10^5, but the *N*-acetyl group has little effect on the reactivity and selectivity of the resulting nitrenium ion.[11] Typically, k_{az}/k_s for the *N*-acetyl ion is only 2- to 10-fold smaller than k_{az}/k_s of the N−H ion, and reaction products are always analogous.[11] The data presented in this paper, along with those previously gathered for **Phe-P-1** and **AαC**, allow us to make comparisons of the reactions of heterocyclic and carbocyclic nitrenium ions, particularly with respect to selectivity for reaction with N_3^- and 2′-deoxyguanosine (d-G). The results also allow us to extend our studies into the range of the highly selective heterocyclic nitrenium ions derived from the strongly mutagenic HCAs.

Results and Discussion

The syntheses of **1a**−**d** are described in the Supporting Information. The **Glu-P** derivatives **1a** and **1b** are stable in the absence of H_2O, but the **IQx** derivatives **1c** and **1d** undergo rearrangement into **4c** and **4d** in nonaqueous solvents, including

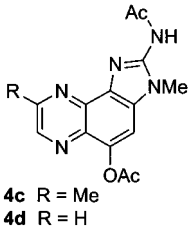

DMF used for stock solutions. Half-lives for rearrangement in DMF at −40 °C were ca. 12−24 h, so fresh stock solutions were prepared daily. Both compounds also underwent slow rearrangement when stored neat at −40 °C so they were synthesized in small batches and used within several days of synthesis.

(4) Novak, M.; Kazerani, S. *J. Am. Chem. Soc.* **2000**, *122*, 3606−3616.
(5) Yamaguchi, K.; Zenda, H.; Shudo, K.; Kosuge, T.; Okamoto, T.; Sugimura, T. *Gann* **1979**, *70*, 849−850.
(6) Kato, T.; Kikugawa, K.; Asanoma, M.; Sakabe, Y. *Mutat. Res.* **1990**, *240*, 259−266.
(7) Manabe, S.; Kanai, Y.; Yanagisawa, H.; Tohyama, K.; Ishikawa, S.; Kitagawa, Y.; Wada, O. *Cancer Res.* **1987**, *47*, 6150−6155.
(8) Hashimoto, Y.; Shudo, K. *Environ. Health Perspect.* **1985**, *62*, 209−214, 215−218.
(9) Turesky, R. J.; Rossi, S. C.; Welti, D. H.; Lay, J. O., Jr.; Kadlubar, F. F. *Chem. Res. Toxicol.* **1992**, *5*, 479−490.
(10) Hashimoto, Y.; Shudo, K.; Okamoto, T. *J. Am. Chem. Soc.* **1982**, *104*, 7636−7640.
(11) (a) Novak, M.; Kahley, M. J.; Lin, J.; Kennedy, S. A.; Swanegan, L. A. *J. Am. Chem. Soc.* **1994**, *116*, 11626−11627. (b) Novak, M.; Lin, J. *J. Org. Chem.* **1999**, *64*, 6032−6040.

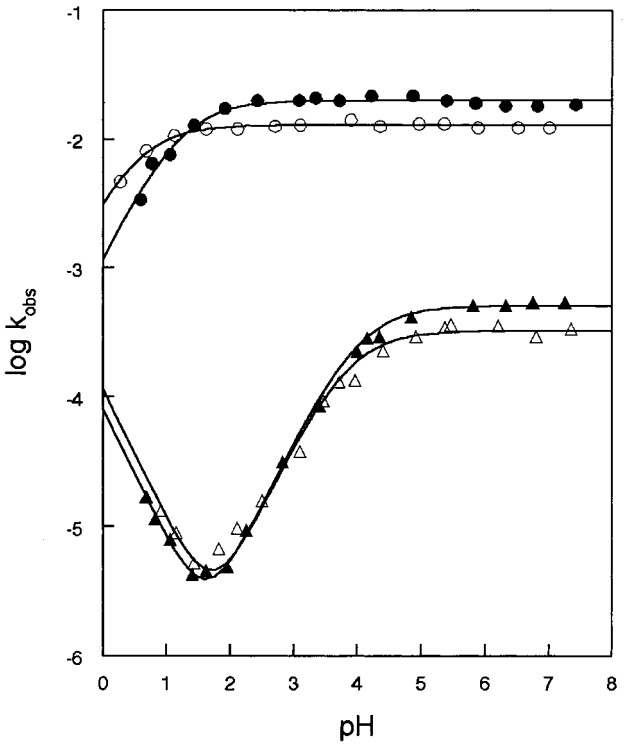

Figure 1. Log k_{obs} vs pH for **1a** (▲), **1b** (△), **1c** (●), and **1d** (○). The lines are the least-squares fit for each data set to eq 1.

The kinetics of the decomposition of **1a**−**d** were monitored at 20 °C by UV or HPLC methods in the pH range from 0.5 to 7.5 in 5 vol % CH_3CN/H_2O at ionic strength 0.5 ($NaClO_4$) in Na_2HPO_4/NaH_2PO_4, NaOAc/HOAc, and $NaHCO_2/HCO_2H$ buffers at pH >2.5 and in $HClO_4$ at pH ≤2.5. Repetitive wavelength scans for **1a** and **1b** showed that isosbestic points held for at least 5 half-lives at pH >1.5, but did not hold at pH ≤1.5, while for **1c** and **1d** isosbestic points held throughout the pH range studied (Supporting Information). It was possible over the entire pH range to monitor the reactions at wavelengths that allowed a good fit of absorbance vs time data to the first-order rate equation for all four compounds. Rate constants were found to be independent of buffer concentration (0.005−0.08 M) or buffer identity, but were dependent on pH (Figure 1 and Supporting Information). Rate constants calculated by initial rates methods from HPLC data confirmed that the rate constants observed at pH ≤1.5 for **1a** or **1b** corresponded to those for their disappearance.

The kinetics were analyzed in terms of the mechanism of Scheme 3 for **1a** and **1b** and a truncated version of that scheme for **1c** and **1d**. The observed rate constants for **1a** and **1b** were fit to eq 1 to obtain the parameters provided in Table 1. For **1c** and **1d** only the second term of eq 1 was necessary to adequately

$$k_{obs} = (k_H(10^{-pH})^2 + K_a k_o)/(K_a + 10^{-pH}) \qquad (1)$$

fit the data. The apparent pK_a values calculated from the kinetic fits corresponded closely (Table 1) to those measured by fitting initial absorbance for **1a**, **1b**, and **1c** vs pH to a standard titration equation. For **1c** this required careful extrapolation back to $t = 0$ because of its rapid decomposition. Spectrophotometric titration was not attempted for **1d**.

The second term of the rate law ($K_a k_o/(K_a + 10^{-pH})$) was observed previously for other ester derivatives of heterocyclic

Scheme 3

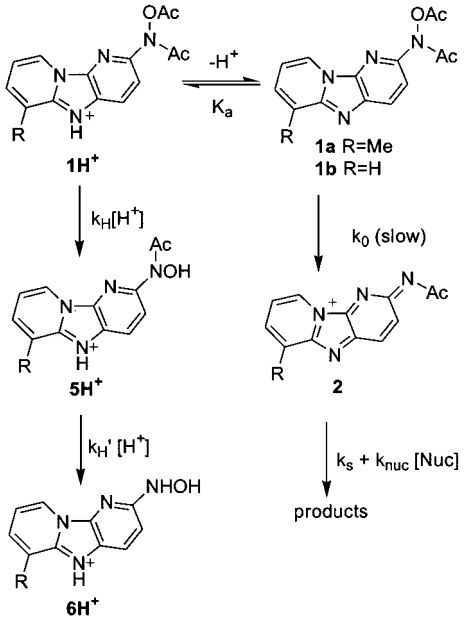

Table 1. Kinetic Parameters for **1a**−**d**[a]

	pK_a			
compd	UV titration	kinetic fit	$10^4 k_o$ (s^{-1})	$10^5 k_H$ (M^{-1} s^{-1})
1a	4.21 ± 0.05	4.04 ± 0.03	5.1 ± 0.2	8.1 ± 0.5
1b	4.17 ± 0.08	3.82 ± 0.06	3.2 ± 0.2	12 ± 1
1c	1.02 ± 0.19	1.21 ± 0.07	199 ± 4	
1d		0.49 ± 0.03	129 ± 2	

[a] Conditions: 5 vol % CH_3CN-H_2O, $T = 20$ °C, $\mu = 0.5$ ($NaClO_4$). Parameters were obtained by a fit to eq 1 or to a standard titration curve.

hydroxylamines.[3,4] The term is consistent with the rate-limiting spontaneous decomposition of the neutral form of the ester to generate a cation that is trapped by solvent or other species in a subsequent fast step (Scheme 3).[3] The value of k_o for **1a** is 1.6-fold greater than that for **1b**, while k_o for **1c** is 1.5-fold greater than that for **1d**. This is consistent with the expected stabilizing effect of the Me substituents on the transition state for formation of the cations.[3,4]

The first term of the rate law ($k_H(10^{-pH})^2/(K_a + 10^{-pH})$) is consistent with acid-catalyzed decomposition of the conjugate acids of **1a** and **1b** (Scheme 3). The site of protonation has not been experimentally determined, but it is expected that N_5 would be the most basic site for **1a** and **1b** based on our observation that the bulky substituents on N_2 would disrupt solvation of protonated N_1.[4] A reasonable explanation of this term would be acid-catalyzed hydrolysis of the ester moiety of **1H**$^+$ to generate the hydroxamic acid as its conjugate acid **5H**$^+$. The hydroxamic acid would undergo hydrolysis under acidic conditions to generate the corresponding hydroxylamine.[12,13] Indeed, **6a** and **6b** are the major observed products of the acid-catalyzed decomposition of **1a** and **1b**, respectively. This is consistent with our observation that authentic **6a** does not undergo the Bamberger rearrangement under these conditions.

The intermediacy of **5a** under acidic conditions was confirmed by a combination of kinetic and HPLC studies. The reaction is

(12) Novak, M.; Bohham, G. A.; Mohler, L. K.; Peet, K. M. *J. Org. Chem.* **1988**, *53*, 3903−3908.
(13) Ghosh, K. K.; Ghosh, S. *J. Org. Chem.* **1994**, *59*, 1369−1374. Ghosh, K. K. *Indian J. Chem.* **1997**, *36B*, 1089−1102.

Table 2. Rate Constants for the Decomposition of **1a** and **5a** Measured in 1.64 M $HClO_4$ at 20 °C

compd	method	$10^5 k_H/[H^+]$ (s^{-1})	$10^4 k_H'/[H^+]$ (s^{-1})
1a	UV (348 nm)	4.6 ± 0.8	1.6 ± 0.3
	HPLC (256 nm)	6.7 ± 0.7	
5a	UV (348 nm)		1.13 ± 0.03
	HPLC (256 nm)		1.19 ± 0.09
5a[a]	HPLC (256 nm)	6.5 ± 0.3	1.4 ± 0.3

[a] These data refer to **5a** detected as an intermediate by HPLC during the decomposition of **1a**.

inconveniently slow in the pH range, but in 1.64 M $HClO_4$ ($H_o = -0.67$)[14] the hydrolysis of **1a** proceeds with a half-life of ca. 3.5 h. Under these conditions the decomposition of **1a** and authentic **5a** were monitored by UV and HPLC methods. At 348 nm the UV data for **1a** were fit to an equation for two consecutive first-order processes. The rate constants collected in Table 2 confirm that one of these processes (k_H) is associated with the decomposition of **1a**, while the other (k_H') is equivalent to the rate constant measured for the decomposition of **5a** under the same conditions. Indeed, **5a** could be detected by HPLC during the decomposition of **1a** under these conditions. Rate constants for its appearance and disappearance, determined by a fit of HPLC peak area vs time data to the consecutive first-order rate equation, match those obtained for authentic **1a** and **5a** (Table 2).

The amines **Glu-P-1** and **Glu-P-2** were also generated as minor reaction products of **1a** and **1b** under acidic conditions (ca. 25%). The source of these products is not known, but control experiments show that the amines were not derived from **5a**,**b** or **6a**,**b** under these conditions.

Although **1c** and **1d** are protonated under acidic pH conditions, they do not exhibit acid-catalyzed hydrolysis at low pH (Figure 1). This appears to be due to their much greater intrinsic reactivity via the nitrenium ion path (k_o for **1c** and **1d** is ca. 40-fold greater than k_o for **1a** and **1b**, respectively) and the smaller pK_a values of their conjugate acids (**1cH**$^+$ and **1dH**$^+$ are ca. 10^3-fold more acidic than **1aH**$^+$ and **1bH**$^+$, respectively). These factors cause **1c** and **1d** to decompose ca. 10^4-fold more rapidly than would **1a** and **1b** at pH <1 via the nitrenium ion pathway. Since the acid-catalyzed hydrolysis pathway for **1c** and **1d** is apparently not accelerated relative to that for **1a** and **1b**, it is not observed in the pH range of this study.

Although rate constants for the decomposition of **1a**−**d** were independent of buffer concentrations in phosphate and acetate buffers, both of these buffers were incorporated into reaction products (Scheme 4). These products were formed with the same rate constants with which **1a**−**d** decomposed (Figure 2). The equilibrium between the acetate products derived from **1a** and **1b**, **9** and **10**, was established rapidly on the time scale of the hydrolysis reaction, but the equilibrium was slow enough that **9** and **10** appeared as separate products during HPLC, although the two peaks tail toward each other. Attempts to isolate pure **9** or **10** by chromatographic methods always led to a mixture of the two isomers. The approximate equilibrium constant, [**10**]/[**9**], was ca. 2 for both **10a** and **9a**, and **10b** and **9b**. The acetate products **4c** and **4d** derived from **1c** and **1d** are the same materials formed by rearrangement of **1c** and **1d**. Fresh stock solutions of **1c** or **1d** contain very little **4c** or **4d**, and the yield

Scheme 4

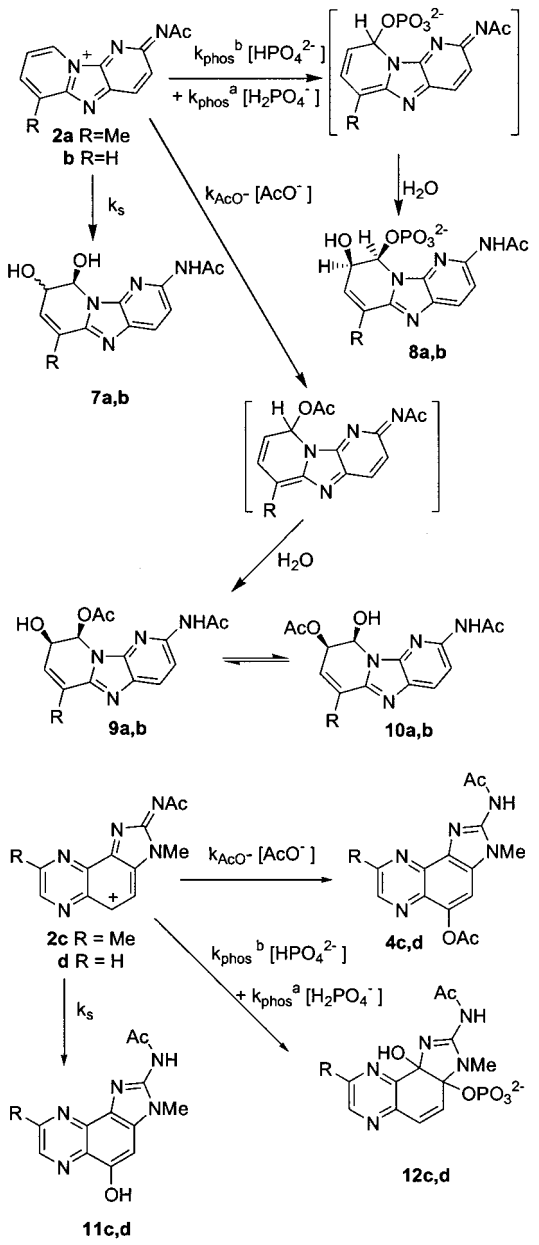

of **4** can be shown to increase with increasing [AcO^-], becoming the only product at high buffer concentrations. These products are not observed in phosphate buffers, confirming their intermolecular origin.

The phosphate adducts **8a** and **8b** were derived from **1a** and **1b**, respectively, while **12c** and **12d** were obtained from **1c** and **1d**, respectively (Scheme 4). Phosphate and acetate adducts were identified primarily by ^{1}H and ^{13}C NMR spectroscopy, including COSY, HSQC, HMBC, and DEPT experiments. The cis-stereochemistry of **8**, **9**, and **10** was established by modeling with MOPAC (AM1) coupled with observed H,H coupling constants for H_7, H_8 and H_8, H_9. One stereoisomer was detected for **12**. The cis-structure (Scheme 4) is assumed. Structural analyses, including stereochemical analyses, are provided in the Supporting Information.

Although only the cis-isomers of **8**, **9**, and **10** were detected, small amounts of the trans-isomers (≤5% of the yields of the cis-isomers) could have escaped detection. Nonetheless, the

(14) Markham, A. E. *J. Am. Chem. Soc.* **1941**, *63*, 874−875. Yates, K.; Wai, H. *J. Am. Chem. Soc.* **1964**, *86*, 5408−5413.

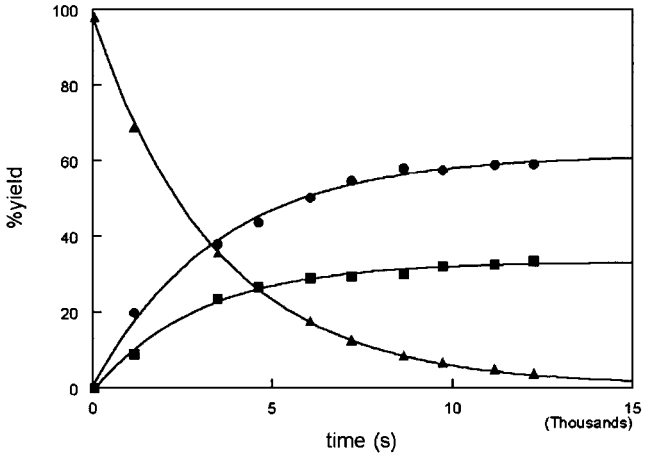

Figure 2. Time course for the disappearance of **1b** (▲) and the appearance of **7b** (●) and **8b** (■) at pH 4.92 in a 0.01 M NaH_2PO_4/Na_2HPO_4 buffer. All data were fit to a first-order rate equation to obtain an average rate constant, k_{obs}, of $(3.0 \pm 0.3) \times 10^{-4}$ s^{-1}. The calculated k_{obs} for **1b** at this pH, based on eq 1 and the data in Table 1, is $(3.0 \pm 0.2) \times 10^{-4}$ s^{-1}.

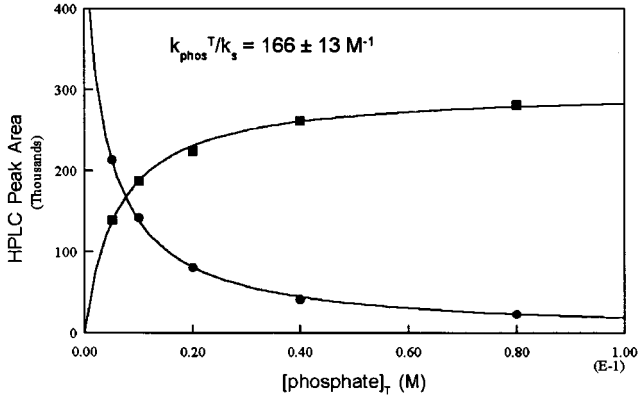

Figure 3. Product yields vs [phosphate]$_T$ for the decomposition of **1b** in pH 6.1 phosphate buffer ($f_b = 0.25$): **7b** (●) and **8b** (■).

Scheme 5

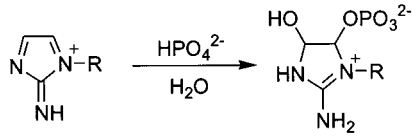

14 **15**

reaction is remarkably diastereoselective for the cis-isomers. The AM1 calculations suggest that the origin of this selectivity is not product stability. The cis-isomers do tend to be more stable than the trans-isomers according to the calculations, but not by sufficient amounts to influence transition state stability to the extent required to account for the results. For example, the heat of formation of the most stable conformer of *cis*-**9b** is calculated to be only 0.84 kcal/mol more negative than the heat of formation of the most stable conformer of *trans*-**9b** at the AM1 level.

In the absence of buffers the 8,9-diol, **7**, is the major product formed from **1a** and **1b**. Only one isomer was detected, but overlapping ^{1}H NMR peaks make assignment of coupling constants problematic. The diol **7** is also subject to decomposition after removal from aqueous solution so detailed structural assignments are difficult to make. The relative stereochemistry at C_8 and C_9 is left unassigned for these reasons. Under all conditions a small amount of the reduction product **13** (ca. 5%) can be detected in reaction mixtures of **1a** and **1b**. The mechanism of the formation of this reduction product is unknown. The diol **7**, as well as **8**, **9**, and **10**, could serve as hydride donors to the cation **2** to generate **13**. Greater yields of **13** were observed under conditions designed for product isolation (ca. 1×10^{-6} to 5×10^{-5} M in **1** for kinetics and HPLC studies, ca. 5×10^{-4} to 1×10^{-3} M for product isolation). Under these conditions higher concentrations of the potential hydride donors are available so increased yields of **13**

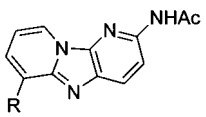

13a R = Me
b R = H

would be expected. The solvent-derived products isolated from the reactions of **1c** and **1d** are **11c** and **11d**. The same products are derived from the spontaneous hydrolysis of **4c** and **4d** that are minor impurities in **1c** and **1d**, but this reaction is slow enough (k_{obs} for **4c** at pH 7 is $(1.0 \pm 0.1) \times 10^{-6}$ s^{-1}) that it does not interfere with product studies performed promptly within 10 half-lives of the decomposition of **1c** (ca. 350 s) or **1d** (ca. 540 s).

Significant reaction of carbocyclic nitrenium ions with acetate or phosphate buffers in buffers of moderate concentration (0.01 M to 0.02 M) has not been observed, but McClelland and coworkers have previously reported that 1-alkyl-2-imidazolylnitrenium ions, **14**, react with phosphate to generate products **15** that are analogous to the phosphate product **12** reported in this study (Scheme 5).[15] In the case of **14** both cis- and trans-products were detected.[15] The structure of **15** and the discovery that the rate of disappearance of **14** generated by laser flash photolysis is dependent on phosphate concentration indicate that **15** is directly generated by attack of phosphate on **14**.[15]

Product studies show that the yields of the phosphate-containing product **8** or **12** are dependent on buffer concentration, and are produced at the expense of the solvent-derived products **7** or **11** as buffer concentrations increase (Figure 3). The instability of **1c** and **1d** complicated product studies, but the problem was overcome by initiating all studies in a given series simultaneously from the same freshly prepared stock solution. The trapping ratio k_{phos}^T/k_s was calculated from the product yield data as a function of total phosphate as previously described for other nucleophiles in the cases of the nitrenium ions derived from **Phe-P-1** and **AαC**.[3,4] These ratios were found to be linearly dependent on the fraction of HPO_4^{2-} in the buffer (Figure 4). The components of the trapping by $H_2PO_4^-$ and HPO_4^{2-} were determined by fitting k_{phos}^T/k_s to eq 2, where k_{phos}^a/k_s is the trapping ratio for $H_2PO_4^-$ and H_2O, k_{phos}^b/k_s is the corresponding ratio for HPO_4^{2-}, and f_b is the fraction of HPO_4^{2-} in the buffer. The trapping ratios are reported in Table 3. The

$$k_{phos}^T/k_s = k_{phos}^a/k_s + (k_{phos}^b - k_{phos}^a)f_b/k_s \qquad (2)$$

results show that HPO_4^{2-} is at least a 10-fold more efficient trap for **2** than its conjugate acid. The ratio k_{AcO^-}/k_s was

Table 3. Rate Constant Ratios for Trapping **2a**−**d** by Phosphate, N_3^-, and d-G[a]

ratio	2a	2b	2c	2d
k_{AcO^-}/k_s (M^{-1})			280 ± 80	
$k_{phos}{}^a/k_s$ (M^{-1})	40 ± 1	58 ± 6	7 ± 4	20 ± 10
$k_{phos}{}^b/k_s$ (M^{-1})	550 ± 5	520 ± 10	520 ± 20	440 ± 50
$k_{az}/k_{phos}{}^b$	$(9.3 \pm 0.2) \times 10^3$	$(4.4 \pm 0.2) \times 10^3$	230 ± 30	120 ± 10
k_{az}/k_s (M^{-1})	$(5.1 \pm 0.1) \times 10^6$	$(2.3 \pm 0.1) \times 10^6$	$(1.2 \pm 0.2) \times 10^5$	$(5.2 \pm 0.5) \times 10^4$
$k_{d-G}/k_{phos}{}^b$	91 ± 4	60 ± 1	1.6 ± 0.5	2.1 ± 0.4
k_{d-G}/k_s (M^{-1})	$(5.0 \pm 0.2) \times 10^4$	$(3.1 \pm 0.1) \times 10^4$	$(8.4 \pm 2.6) \times 10^2$	$(9.1 \pm 2.1) \times 10^2$

[a] Rate constant ratios are defined in the text or in Schemes 4 and 6.

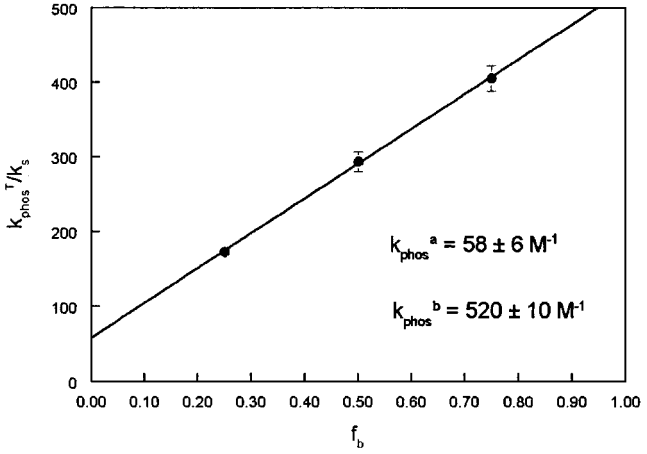

Figure 4. $k_{phos}{}^T/k_s$ vs f_b for **1b** in phosphate buffer.

calculated for **2c** by monitoring the yield of **4c** as a function of [AcO^-] in pH 4.8 acetate buffer. That value is also included in Table 3.

The cations **2a**−**d** are trapped by N_3^- and 2′-deoxyguanosine, d-G. Products are summarized in Scheme 6. These products are formed in phosphate concentrations sufficiently high to swamp out the solvent-derived products (0.02−0.20 M). The yields of N_3^- trapping products exceed 95% in 0.02 M pH 6.9 Na_2HPO_4/NaH_2PO_4 buffer at [N_3^-], well below 0.01 M for all four cations. The d-G trapping is less efficient, but still exceeds 70% of reaction products at 0.02 M d-G under these buffer conditions for all four ions. This trapping occurs without rate acceleration (Table 4). The rate constant ratios k_{az}/k_s and k_{d-G}/k_s can be obtained indirectly by monitoring product yields as a function of nucleophile concentration in buffers of constant phosphate concentration sufficiently high that the yield of **7** or **11** is insignificant (Figure 5). The ratio of second-order rate constants $k_{az}/k_{phos}{}^b$ or $k_{d-G}/k_{phos}{}^b$ can be determined from these data since [HPO_4^{2-}] is constant and the reactions are run under buffer conditions in which the contribution of $H_2PO_4^-$ is negligible. The nucleophile/solvent selectivities can then be obtained by multiplication. The rate constant ratios are summarized in Table 3. The values of k_{az}/k_s are somewhat larger for the Me-substituted cations **2a** or **2c** than for **2b** or **2d**, respectively. The higher N_3^-/solvent selectivity of **2a** and **2c** is expected if k_{az} is diffusion limited because those ions should react with solvent more slowly than their unsubstituted analogues.

Scheme 6

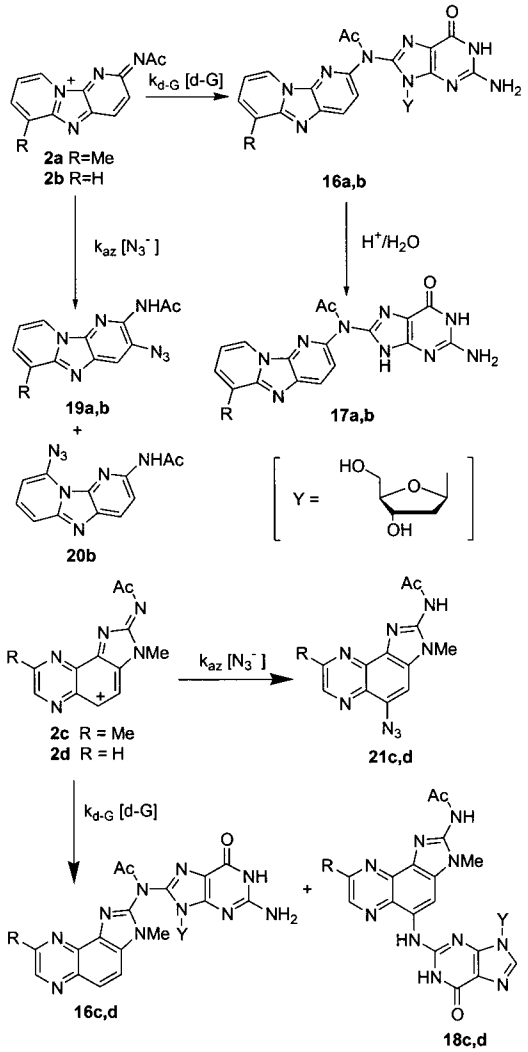

Alternatively, $k_{az}/k_{phos}{}^b$ can also be obtained by monitoring product yields as a function of [HPO_4^{2-}] at constant [N_3^-] sufficiently high that the solvent-derived product is not observed. This was done for **1b** to obtain $k_{az}/k_{phos}{}^b$ of $(5.3 \pm 1.1) \times 10^3$. The resulting value of k_{az}/k_s ($(2.7 \pm 0.4) \times 10^6\ M^{-1}$) is in good agreement with the value reported in Table 3.

The C-8 adducts **16** are generated by the reaction of all four cations with d-G. These adducts are analogous to those identified from the reaction of other heterocyclic and carbocyclic nitrenium ions with d-G.[3,4,16] They are the most commonly identified DNA

(15) McClelland, R. A.; Panicucci, R.; Rauth, A. M. *J. Am. Chem. Soc*. **1985**, *107*, 1762−1763. McClelland, R. A.; Panicucci, R.; Rauth, A. M. *J. Am. Chem. Soc*. **1987**, *109*, 4308−4314. Bolton, J. L.; McClelland, R. A. *J. Am. Chem. Soc*. **1989**, *111*, 8172−8181. Gadosy, T. A.; McClelland, R. A. *J. Am. Chem. Soc*. **1999**, *121*, 1459−1465.

(16) (a) Novak, M.; Kennedy, S. A. *J. Am. Chem. Soc*. **1995**, *117*, 574−575. (b) Kennedy, S. A.; Novak, M.; Kolb, B. A. *J. Am. Chem. Soc*. **1997**, *119*, 7654−7664. (c) McClelland, R. A.; Ahmad, A.; Dicks, A. P.; Licence, V. E. *J. Am. Chem. Soc*. **1999**, *121*, 3303−3310.

Table 4. Rate Constants for the Decomposition of **1a**−**d** in the Presence and Absence of N_3^- and d-G

conditions	$10^4 k_{obs}$ (s^{-1}) 1a	1b	1c	1d
no added nucleophile[a]	5.35 ± 0.01	3.28 ± 0.15	205 ± 4	121 ± 4
0.01 M N_3^- [b]	5.99 ± 0.03	3.75 ± 0.32	195 ± 6	142 ± 2
0.01 M d−G[c]	5.14 ± 0.04	3.21 ± 0.02		
0.02 M d−G[d]			180 ± 9	107 ± 4

[a] Conditions: 5 vol % CH_3CN-H_2O, $T = 20$ °C, $\mu = 0.5$ ($NaClO_4$) in 0.02 M 2/1 Na_2HPO_4/NaH_2PO_4 buffer, pH 6.9. [b] Calculated % trapping by N_3^- exceeds 98% for **2a**−**d**. [c] Calculated % trapping by d-G exceeds 97% for both **2a** and **2b**. [d] Calculated % trapping by d-G exceeds 70% for both **2c** and **2d**.

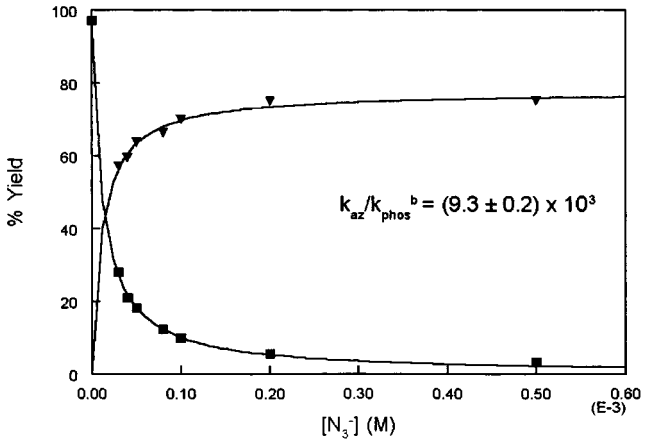

Figure 5. Product yields for **8a** (■) and **19a** (▼) as a function of $[N_3^-]$ during the decomposition of **1a**. Buffer conditions are the following: 0.16 M phosphate buffer, $f_b = 0.67$, pH 6.9.

adducts from in vitro and in vivo experiments involving the amines or their metabolites.[1,8] The adducts **16a**,**b** are stable at neutral pH, but are subject to hydrolysis of the C−N glycosidic bond under acidic pH conditions to generate **17a**,**b**. The hydrolytic stability of **16c**,**d** was not examined. In addition, **2c**,**d** also generate the unusual N-2 adducts **18c**,**d**. Only C-8 adducts have previously been reported from the reactions of most heterocyclic and carbocyclic esters with monomeric d-G,[3,4,16] but **MeIQx** and **IQ** derivatives have been shown to generate both C-8 and N-2 adducts from reaction with monomeric d-G.[9] Typically N-2 adducts are reported for most ester derivatives of *N*-arylhydroxylamines only when they react with native DNA.[17] The C-8/N-2 adduct ratio is 3.5/1.0 for **2c**. The C-8/N-2 ratio observed for the reaction of **NOHMeIQx** with d-G in the presence of Ac_2O in 0.1 M pH 7.0 phosphate buffer was 11/1.[9] The reported C-8/N-2 ratio in calf thymus DNA treated similarly is 5.2/1, indicating that formation of the N-2 adduct is more favorable in DNA than in d-G even for the IQ type HCAs.[9]

The reactions of **2a**−**d** with phosphate and acetate to produce the addition products **8**, **9**, **10**, and **12** are unusual, and suggest that **2a**−**d** behave differently from most carbocyclic nitrenium ions, but **2a**−**d** still possess sufficient nitrenium ion character to react with d-G at the exocyclic N. Additionally, both **2a** and **2b** are efficiently reduced by I^- to generate **13a** and **13b**, respectively. This is another characteristic reaction of nitrenium ions.[18]

The N_3^- adducts **19**, **20**, and **21** are also characteristic substitution products similar to those previously reported for other heterocyclic and carbocyclic nitrenium ions.[3,4,11,19] Both **2a** and **2b** generate the 3-N_3 product **19**, but only **2b** gives a detectable yield of the 9-N_3 product **20b** in the N_3^- concentration range used in our product studies (5×10^{-6} to 2×10^{-3} M).

The dependence of the yields of **19b** and **20b** on $[N_3^-]$ (Supporting Information) suggests that the initial addition intermediates produced by attack of N_3^- on C_9 or C_3 of **2b** can yield either final product. A significant portion of the yield of **20b** is apparently generated at the expense of **19b** at higher $[N_3^-]$, and the yield of **19b** decreases from a high of around 82% at 6×10^{-5} M N_3^- to about 68% at $[N_3^-] > 1 \times 10^{-3}$ M. The yield of **19b** remains constant at that level up to at least 2×10^{-2} M N_3^-. A quantitative fit of the product yield data, provided in the Supporting Information, suggests that ca. 67% of the initial attack on **2b** occurs on C_9. The C_3 product, **19b**, predominates at all $[N_3^-]$ because the addition intermediate derived from attack of N_3^- on C_9 preferentially generates **19b** even at very low $[N_3^-]$. No product equivalent to **20b** was detected during the N_3^- trapping studies of **2a**, but at very high N_3^- concentrations ($[N_3^-] \geq 0.01$ M) small amounts of the diazide product **22a** were detected. This shows that attack at C_9 also occurs for **2a**, although the extent of such attack cannot be quantitatively assessed.

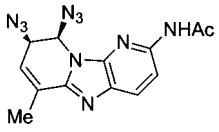

22a

N_3^- attack on most carbocyclic nitrenium ions such as *N*-acetyl-4-biphenylylnitrenium ion, **23a**, and *N*-acetyl-2-fluorenylnitrenium ion, **24a**, occurs predominately at a position ortho to the nitrenium ion center if the para position is blocked.[19,20] The apparent predominant attack of N_3^- on **2b** at C_9 shows that the regiochemistry of trapping reactions on heterocyclic nitrenium ions can be profoundly affected by the structure of the heterocyclic ring. The ions **2a** and **2b** in several of their reactions behave more like highly conjugated iminium ions than as typical nitrenium ions. This tendency to react with N_3^- at conjugated sites other than the ortho carbon is also shared with the *N*-acetyl-4-stilbenylnitrenium ion, **25**, that reacts with N_3^- predominately at the β-vinyl carbon (85%) with only a minor amount of reaction occurring at the ortho carbon (13%).[21] This ion also reacts with H_2O to generate 1,2-diol products across the α- and β-vinyl carbons much like those observed for **2a** and **2b**, but it did not react significantly with AcO^- or HPO_4^{2-}.[21]

The N_3^- trapping data provide a lower limit for the lifetime of **2a**−**d** in aqueous solution since k_{az} cannot exceed the diffusion limit of ca. 5×10^9 M^{-1} s^{-1} established for a wide

(17) Kriek, E. *Cancer Res.* **1972**, *32*, 2042−2048. Westra, J. G.; Kriek, E.; Hittenhausen, H. *Chem.-Biol. Interact.* **1976**, *15*, 149−164. Kriek, E.; Hengeveld, G. M. *Chem.-Biol. Interact.* **1978**, *21*, 179−201. Meerman, J. H. N.; Beland, F. A.; Mulder, G. J. *Carcinogenesis* **1981**, *2*, 413−416. Beland, F. A.; Dooley, K. L.; Jackson, C. D. *Cancer Res.* **1982**, *42*, 1348−1354.

(18) Pelecannou, M.; Novak, M. *J. Am. Chem. Soc.* **1985**, *107*, 4499−4503.

(19) Novak, M.; Kahley, M. J.; Eiger, E.; Helmick, J. S.; Peters H. E. *J. Am. Chem. Soc.* **1993**, *115*, 9453−9460.

(20) (a) Davidse, P. A.; Kahley, M. J.; McClelland, R. A.; Novak, M. *J. Am. Chem. Soc.* **1994**, *116*, 4513−4514. (b) Novak, M.; Kahley, M. J.; Lin, J.; Kennedy, S. A.; James, T. G. *J. Org. Chem.* **1995**, *60*, 8294−8304.

(21) Novak, M.; Kayser, K. J.; Brooks, M. E. *J. Org. Chem.* **1998**, *63* 5489−5496.

Table 5. Comparison of $\log(k_{az}/k_s)$ and $\log(k_{d-G}/k_s)$ for Carbocyclic and Heterocyclic Nitrenium Ions[a]

ion	$\log(k_{az}/k_s)$	$\log(k_{d-G}/k_s)$
2a[b]	6.71	4.70
2b[b]	6.36	4.49
2c[b]	5.08	2.92
2d[b]	4.72	2.96
23a[c]	2.97	2.51
23b[d]	3.45	3.04
23c[e]	2.89	2.15
23d[e]	3.60	2.94
23e[e]	3.50	2.88
23f[e]	3.79	3.11
23g[e]	3.85	3.18
23h[e]	4.53	3.75
23i[e]	6.59	4.36
24a[f]	4.76	3.88
24b[g]	5.07	4.46
26a[h]	2.73	≤0.65
26b[i]	3.68	≤1.26
27[j]	2.48	1.92
28a[k]	4.65	3.94
28b[k]	4.54	3.91

[a] Conditions: 5 vol % CH_3CN-H_2O, $\mu = 0.5$, $T = 20$ °C, unless otherwise specified. Multiple measurements by different methods were averaged. [b] Source: this work. [c] Source: refs 16b, 19, 20a, and 24. [d] Source: refs 16b, 19, 22a, and 24. [e] Source: refs 23 and 24. Conditions: 20 vol % CN_3CN-H_2O, $\mu = 0$. [f] Source: refs 11a, 16b, 20a, and 24. [g] Source: refs 22a and 24. [h] Source: ref 11a and unpublished results. [i] Source: ref 22c. Condition: H_2O. [j] Source: ref 3. [k] Source: ref 4.

range of other nitrenium ions under these conditions.[20,22] The k_{az}/k_s ratios for **2a** and **2b** are at the upper limit of those observed for carbocyclic nitrenium ions that have k_{az} at or near the diffusion limit,[23] so it is possible that k_{az} for **2a** and **2b** is significantly below 5×10^9 M^{-1} s^{-1}. Nevertheless, the estimated lifetimes, $1/k_s$, for **2a** and **2b** of 1.0 and 0.5 ms, respectively, show that these are quite stabilized cations capable of high selectivity in their reactions with nucleophiles because of their long aqueous solution lifetimes. The estimated lifetimes of **2c** and **2d** of 24 and 10 μs, respectively, are in the same range as those for **24a** and **24b**, both of which react with N_3^- at or near the diffusion-controlled limit.[20a,22a] These are also quite stabilized nitrenium ions, although less stable than **2a**,**b**, and the highly stabilized **23i**.[23,24]

Table 5 provides a comparison of $\log(k_{az}/k_s)$ and $\log(k_{d-G}/k_s)$ for **2a**−**d** with a series of carbocyclic and heterocyclic ions **23**−**24** and **26**−**28** identified in Scheme 7. The data were obtained either by competition studies similar to those described here or by direct measurements of rate constants on nitrenium ions generated by laser flash photolysis.[3,4,11,16,19,20,22−24] A plot of $\log(k_{d-G}/k_s)$ vs $\log(k_{az}/k_s)$ (Figure 6) shows that **2a**−**d** and several other ions exhibit 1 to 2 orders of magnitude lower selectivity toward d-G than predicted by the correlation line for the majority of the ions. The data points for those ions fall on a line of unit slope that would be expected if both k_{az} and k_{d-G} are diffusion limited. In fact, for the ions that fall on the line, measured values of k_{az} do cluster around 5×10^9 M^{-1} s^{-1} at $\mu = 0.5$ and 1×10^{10} M^{-1} s^{-1} at $\mu = 0.0$, while k_{d-G} is ca. $(1-2) \times 10^9$ M^{-1} s^{-1} at $\mu = 0.0$ or 0.5.[16,20,22−24] These are

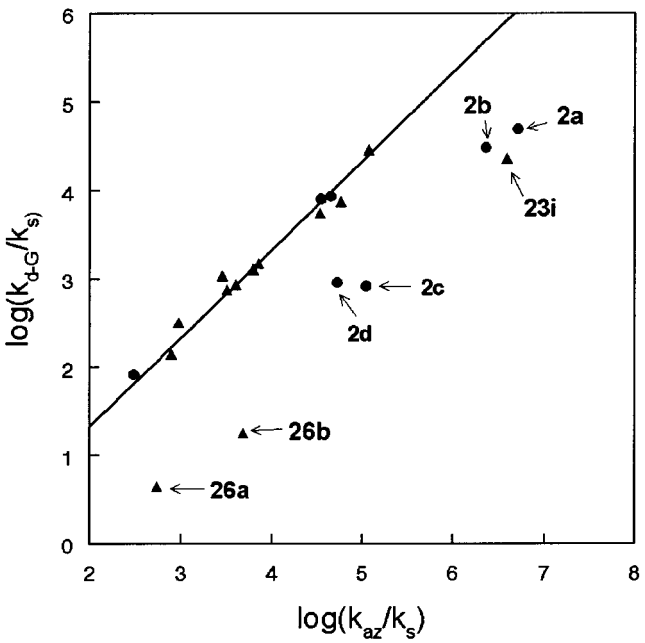

Figure 6. Log (k_{d-G}/k_s) vs $\log(k_{az}/k_s)$ for heterocyclic (●) and carbocyclic (▲) nitrenium ions that exhibit reactivity with C-8 of d-G. The correlation line is $\log(k_{d-G}/k_s) = \log(k_{az}/k_s) - 0.67$. Ions that fall off the line are identified.

Scheme 7

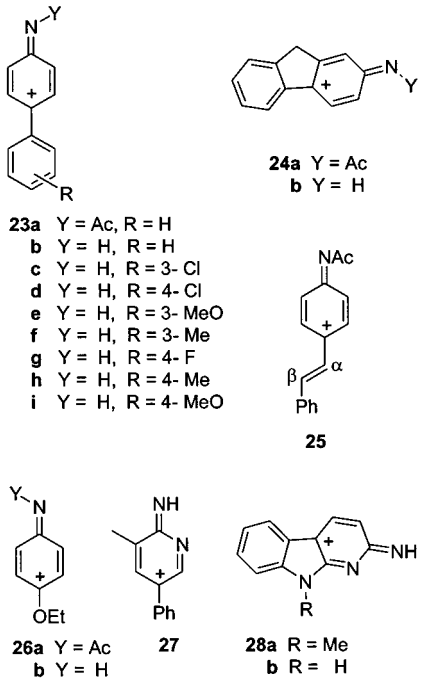

considered to be the diffusion-controlled limits for these reactions. Measured values of k_{az} for two of the ions that fall below the line (**23i** and **26b**) are within a factor of 2 of the apparent diffusion limits, so the points that fall significantly below the line apparently do so because k_{d-G} is 1 to 2 orders of magnitude below the diffusion limit for those ions. The onset of activation-limited reactions with d-G is not related to the magnitude of k_s for these ions, since the ions that fall significantly below the line have k_s ranging from ca. 10^3 to 10^7 s^{-1}. McClelland has suggested that the activation-limited reaction of certain nitrenium ions with d-G is related to the ability of substituents in the ions to localize the positive charge

(22) (a) McClelland, R. A.; Davidse, P. A.; Hadzialic, G. *J. Am. Chem. Soc.* **1995**, *117*, 4173−4174. (b) Bose, R.; Ahmad, A. R.; Dicks, A. P.; Novak, M.; Kayser, K. J.; McClelland, R. A. *J. Chem. Soc., Perkin Trans. 2* **1999**, 1591−1599. (c) Ramlall, P.; McClelland, R. A. *J. Chem. Soc., Perkin Trans. 2* **1999**, 225−232.
(23) Ren, D.; McClelland, R. A. *Can J. Chem.* **1998**, *76*, 78−84.
(24) McClelland, R. A.; Gadosy, T. A.; Ren, D. *Can. J. Chem.* **1998**, *76*, 1327−1337.

Scheme 8

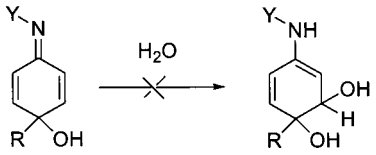

29

on a heteroatom other than the nitrenium N.[22c] It was argued that this would reduce the electrophilic reactivity at the nitrenium N necessary for formation of the C-8 adduct. All seven of the ions that fall below the correlation line do have a dominant resonance structure in which the charge is localized onto a heteroatom (O or N) with all heavy atoms maintaining an octet of electrons, but so do two of the ions that fall on the line (**28a**,**b**).

If k_{az} is diffusion limited for **2a**−**d**, k_{d-G} for all four cations is in the range of $(4-9) \times 10^7$ M^{-1} s^{-1}. The relatively slow trapping of these ions by d-G may play a role in the detection of the N-2 adducts, **18c**,**d**. If the reaction of **2c** with d-G to form the C-8 adduct did proceed at the diffusion-controlled limit, while the rate constant for formation of the N-2 adduct remained unchanged, the relative yield of **18c** would be ca. 1% rather than the observed 22%.

The results obtained for the heterocyclic nitrenium ions **2a**−**d**, **27**, **28a**, and **28b** show that these ions retain many of the characteristic reactions of carbocyclic nitrenium ions: selective reaction with N_3^- to generate substitution products, reaction with d-G to form C-8 adducts, and efficient reduction by I^-. The more stable ions **2a**−**d** exhibit unusual reactions with HPO_4^{2-} or AcO^- to generate addition products in which the aromatic character of one or more rings is lost.

In carbocyclic ions typically only H_2O reacts to form stable addition products in which aromaticity is lost. This occurs presumably because of the poor leaving group ability of OH^- in products such as **29**.[20b] Attack of a second equivalent of H_2O (Scheme 8) is kinetically disfavored at moderate pH (except for **25** and related stilbenyl ions) because such reactions appear to require specific acid catalysis and do not lead to products stabilized by recovery of aromatic character.[20b] Apparently the aromatic character of the heterocyclic rings of **2a**−**d** is considerably weaker allowing better leaving groups such as HPO_4^- and AcO^- to form addition products (Scheme 4) that do not revert to the nitrenium ion. Attack of H_2O on the inital addition product to form products such as **7**, **8**, **9**, **10**, and **12** is more favorable in these cases because there is less driving force for rearomatization.

Experimental Section

Synthesis. The syntheses of **Glu-P-1**, **Glu-P-2**, **MeIQx**, **IQx**, and the nitro derivatives **NO_2Glu-P-1, NO_2Glu-P-2, NO_2MeIQx**, and **NO_2IQx** have been described in the literature.[25,26] The hydroxylamines **NOHGlu-P-1**, **NOHGlu-P-2**, **NOHMeIQx**, and **NOHIQx** were synthesized by the method of Kazerani and Novak by N_2H_4 reduction of the nitro compounds.[27] The esters **1a**−**d** were prepared, as described in the Supporting Information, by reacting the hydroxylamines with 2 equiv of AcCl in THF. The hydroxamic acid **5a** was obtained by basic hydrolysis of **1a** in THF/H_2O as described in the Supporting Information.

Kinetic and Product Studies. Purification of solvents and general procedures for performing kinetic studies, product studies by HPLC methods, and data handling have been described.[19,28] All reactions were performed in 5 vol % CH_3CN-H_2O at an ionic strength of 0.5 maintained with $NaClO_4$ except for those reactions that occurred in 1.64 M $HClO_4$. Buffers used to maintain pH were Na_2HPO_4/NaH_2PO_4, NaOAc/HOAc, or HCOONa/HCOOH. At pH ≤2.5 $HClO_4$ solutions were used. Initial concentrations of **1a**−**d** of ca. 5×10^{-5} M for kinetics and product studies were obtained by 15 μL injection of a 0.01 M stock solution in DMF into 3.0 mL of the solution that had been incubated at 20 °C for 15 min. Repetitive wavelength scans were collected between 200 and 400 nm for at least 5 half-lives of the reaction. Absorbance vs time data for **1a** were collected at 256 (pH 0.8−4.4) and 263 nm (pH 4.8−7.4). For **1b** data were collected at 252 (pH 0.9−3.7) and 262 nm (pH 3.9−7.4). Kinetic data for **1c** and **1d** were collected at 266 nm at all pH values. Data were fit to the first-order rate equation to obtain k_{obs}.[28] Rate constants for the disappearance of **1a** were also determined in acidic solutions by the initial rates method, using HPLC with UV detection at 256 nm. Spectrophotometric titrations were carried out at 257 nm for **1a**, 255 nm for **1b**, and 266 nm for **1c**. Kinetics of decomposition of **1a**−**d** in the presence of N_3^- and d-G were performed in 0.02 M 2/1 Na_2HPO_4/NaH_2PO_4 buffers at pH 6.90. These reactions were followed at the following wavelengths: **1a**, 323 (N_3^-) and 314 nm (d-G); **1b**, 272 (N_3^-) and 316 nm (d-G); and **1c** and **1d**, 266 (N_3^-) and 335 nm (d-G).

Reaction products of **1a** and **1b** in phosphate and acetate buffers and in $HClO_4$ solutions were monitored by HPLC on a C_8 reverse-phase analytical column with UV detection at 320 nm, using 50/50 MeOH/H_2O eluent buffered with 0.05 M 1:1 NaOAc/HOAc at a flow rate of 1 mL/min. Product yields were determined by triplicate 20 μL injections after 10 half-lives of the reaction. Identical conditions were used for **1c** and **1d** except that products were monitored at 300 nm and the eluting buffer was 40/60 MeOH/H_2O. For the determination of k_{phos}^T/k_s selectivity ratios, 0.08 M phosphate buffers were made with varying buffer ratios. These buffers were diluted to 0.04, 0.02, 0.01, and 0.005 M while maintaining the ionic strength. After 10 half-lives of the reaction, product yields were determined by HPLC methods.

Details of the isolation and characterization of the buffer and solvent-derived products **4c**,**d**, **7a**,**b**, **8a**,**b**, **9a**,**b**, **10a**,**b**, **11c**,**d**, and **12c**,**d** are described in the Supporting Information.

Product Studies in the Presence of N_3^- and d-G. All buffers were Na_2HPO_4/NaH_2PO_4 (B/A = 2/1; pH 6.9), $\mu = 0.5$, 5 vol % CH_3CN/H_2O. All reactions were carried out at 20 °C. The buffer solutions had been incubated at 20 °C for 15 min prior to the addition of **1a**−**d**. The product yields were determined by HPLC (UV detection at 256, 300, and 320 nm, using 50/50 or 40/60 MeOH/H_2O eluent buffered as described above).

The product yields for **1a** in N_3^- solutions were determined in 0.16 M total buffer with N_3^- concentrations ranging from 3×10^{-5} to 5×10^{-4} M. The initial concentration of **1a** was ca. 5×10^{-6} M, which was obtained by 15 μL injections of a 0.001 M stock solution in DMF into 3.0 mL of the buffer solution. The product yields were determined by HPLC as described above.

The N_3^- selectivity ratio for **1b** was determined by two methods: (1) varying phosphate concentrations while maintaining constant azide concentration and (2) varying azide concentrations while maintaining constant phosphate concentration. (1) Buffers were prepared with 0.02−0.16 M total phosphate, and constant 5×10^{-6} M N_3^-. The initial

(25) Takeda, K.; Shudo, K.; Okamoto, T.; Kosuge, T. *Chem. Pharm. Bull.* **1978**, *26*, 2924−2925. Hashimoto, Y.; Shudo, K.; Okamoto, T. *J. Am. Chem. Soc.* **1982**, *104*, 7636−7640. Bristow, N. W.; Charlton, P. T.; Peak, D. A.; Short, W. F. *J. Chem. Soc.* **1954**, 616−629. Astik, R. R.; Thaker, K. A. *J. Ind. Chem. Soc.* **1981**, *58*, 1013−1014. Saint-Ruf, G.; Loukakou, B.; N'Zouzi, C. *J. Heterocycl. Chem.* **1981**, *18*, 1565−1570.
(26) Grivas, S.; Olsson, K. *Acta Chem. Scand.* **1985**, *B39*, 31−34. Grivas, S. J. *Chem. Res.* **1988**, 84.
(27) Kazerani, S.; Novak, M. *J. Org. Chem.* **1998**, *63*, 895−897.
(28) Novak, M.; Pelecanou, M.; Roy, A. K.; Andronico, F. M.; Plourde, F. M.; Olefirowicz, T. M.; Curtin, T. J. *J. Am. Chem. Soc.* **1984**, *106*, 5623−5631.

concentration of **1b** was ca. 1.0×10^{-6} M. (2) Buffers with constant 0.02 M buffer and 5×10^{-6}−2×10^{-3} M NaN_3 were prepared. The initial concentration of **1b** was ca. 1×10^{-6} M. This concentration was obtained by 15 μL injection of a 2×10^{-4} M stock solution in DMF into 3.0 mL of the buffer solution. The product yields were determined by HPLC.

Procedures for **1c** and **1d** were similar to those followed for **1a** except that initial concentrations of the esters were kept at ca. 1×10^{-5} M. The concentration range of N_3^- in these studies was 5×10^{-5}−1×10^{-3} M. Decomposition reactions of **1a**−**d** in d-G containing solutions were carried out in phosphate buffers with 0.02 M total buffer concentration. Reaction products were monitored by HPLC with UV detection at 300 or 320 nm as described above.

Details of the large-scale isolation and characterization of the N_3^- and d-G adducts **16a**−**d**, **18c**,**d**, **19a**,**b**, **20b**, **21c**,**d**, and **22a** are described in the Supporting Information.

Calculations

The AM1 semiempirical calculations were carried out on a Dell Optiplex GX200 desktop computer with an Intel Pentium III processor and 256 MB RAM, using CambridgeSoft MOPAC Pro 5.0 software. The lowest energy conformation of **9b** in both the cis- and trans-configurations was found by energy minimization starting from several different conformations of the 2-acetamido and the 9-O-acetyl groups. The lowest energy conformation of *cis*- and *trans*-**8b** was found by substituting the 9-*O*-acetyl groups in the lowest energy conformations of *cis*-**9b** and *trans*-**9b** with a 9-phosphoryl group and minimizing the energy of the molecule. Heats of formation vs dihedral angle calculations were generated by energy minimizations of *cis*-**9b** and *trans*-**9b** with fixed N_{10}−C_9−O_9−C_{9OAc} dihedrals initially at 10° intervals.

Acknowledgment. This work was supported by a grant from the American Cancer Society (RPG-96-078-03-CNE). NMR spectra were obtained on equipment made available through an NSF grant (CHE-9012532) and upgraded through an Ohio Board of Regents Investment Fund grant. MALDI-TOF and LC-MS mass spectra were obtained on equipment funded by the NSF (CHE-9413529) and the Ohio Board of Regents Investment Fund, respectively. High-resolution mass spectra were obtained at the Ohio State University Chemical Instrumentation Center.

Supporting Information Available: Synthesis of **1a**−**d** and **5a**, table of rate constants obtained for the decomposition of **1a**−**d**, isolation and characterization of the buffer and solvent derived products **4c**,**d**, **7a**,**b**, **8a**,**b**, **9a**,**b**, **10a**,**b**, **11c**,**d**, and **12c**,**d**, and the N_3^- and d-G adducts **16a**−**d**, **18c**,**d**, **19a**,**b**, **20b**, **21c**,**d**, and **22a**, kinetic analysis of the N_3^- dependence of the yields of **19b** and **20b**, and repetitive wavelength scans for **1a**−**d** (PDF). This material is available free of charge via the Internet at http://pubs.acs.org.

JA0121944